JOURNAL OF MATERIALS SCIENCE **34** (1999) 5315–5323

Pore size tailorability in γ Al_2O_3 membranes using surfactant micelles as templates

M. SINGH, M. K. TRIVEDI, J. BELLARE
Microstructure Engineering Laboratory, Chemical Engineering Department, IIT-Bombay, Powai, Mumbai 400076
E-mail: jb@che.iitb.ernet.in

γ Al_2O_3 membranes with highly tailorable pore sizes in the range of 50–60 Å could be prepared by using surfactant micelles of varying sizes as templates. Surfactants were incorporated in the alumina sol by dissolving them in water above their critical micellar concentration and using the micellar solutions to hydrolyze aluminium alkoxides. 15 mM solutions of quaternary ammonium surfactants namely dodecyl trimethyl ammonium bromide, tetradecyl trimethyl ammonium bromide, and hexadecyl trimethyl ammonium bromide were found to give pore sizes of 50, 55 and 60 Å respectively as obtained by nitrogen adsorption BET and transmission electron microscopy (TEM) methods. These pore sizes also match closely with the micellar sizes obtained by quasi elastic light scattering measurements. Moreover, it was also found that the total pore volume increases with increase of the amount of surfactant. Rejection of standard polyethylene glycol (PEG) solutions of different molecular weights as well as some globular protein solutions of different molecular weights was determined in these membranes and the data were explained on the basis of the model originally developed by Sourirajan and Matsuura and later modified by Brites and de Pinho.

Nomenclature

b	friction function defined by $b = (f_{sw} + f_{sm})/f_{sm}$
c	solute concentration (g/cm^3)
C_s	solute concentration (kg/m^3)
C_{sb}	bulk solute concentration (kg/m^3)
C_{sm}	solute concentration at the membrane wall (kg/m^3)
C_{sp}	permeate solute concentration (kg/m^3)
D_{sw}	diffusivity of solute in water (m^2/s)
f_{sw}	proportionality constant relating the friction force between solute and pore wall to the velocity difference between solute and pore wall (J s/m mol)
f_{sm}	proportionality constant relating the friction force between solute and pore wall to the velocity difference between solute and pore wall (J s/m mol)
F_s	diffusion force (mol/m^2 s Pa.)
$F_{surface}$	Permeability due to surface flow (mol/m^2 s Pa.)
F_{sw}	friction force between solute and solvent (J s/m mol)
F_{sm}	friction force between solute and pore wall (J s/m mol)
$F(R_p)$	pore size distribution function
J_v	volumetric flux (m/s)
k_0	tortuosity factor
L	thickness of the membrane or length of a pore (m)
p	feed pressure (kPa)
r	radial distance in cylindrical coordinate set in membrane pore (m)
R	gas constant (m^3 atm/mol K)
R'	rejection (%)
$\underline{R}_p$	pore radius (m)
R_p	average pore radius (m)
T	absolute temperature (K)

Greek symbols

α	dimensionless velocity defines as $\alpha(\rho) = v_w(r)L f_{sw}/RT$
σ	standard deviation for pore size distribution
ε	porosity of the membrane
ρ	dimensionless quantity defined as r/R_p
ρ_d	true density of the solid (kg/m^3)

1. Introduction

Microporous and mesoporous ceramics with pore sizes in the range of 10–500 Å have gained considerable importance in the last few years for uses as catalysts and sorption media and as membranes for separation. The growing interest in this field has resulted in the need for a very precise control of pore sizes in these materials, particularly for mesoporous ones with pore diameters ranging between 20 and 100 Å. In the microporous range, i.e. less than 15 Å, zeolites are still the best examples of materials exhibiting a highly ordered and narrowly distributed pore structure.

The first attempts to make mesoporous ceramic materials with a high degree of order and narrow distribution of pore sizes was made by Kresge *et al.* [1] of Mobil Oil Corporation. These materials designated as MCM 41 were first observed in electron micrographs of products from hydrothermal reaction of alumino-silicate gel in the presence of quaternary surfactants. The material was found to possess regular arrays of uniform channels, the dimensions of which can be tailored with the suitable choice of surfactant. Thereafter, other workers e.g. Stucky *et al.* [2], and Tanev and Pinnavaia [3] have worked on making mesoporous silicas by the surfactant templating route using the sol-gel process. However, work on mesoporous aluminas or membranes of such materials have not been reported in literature so far.

In the present work γ alumina thin films were prepared using a similar strategy. Surfactant micelles were incorporated in the boehmite (γ AlOOH) sol prepared by the usual Yoldas process [4] and this was further used for making thin film membranes by coating, drying, and firing subsequently. When alumina gels were fired at 600 °C the surfactant molecules burned out leaving pores characteristic of their sizes in the parent material. It was found that the average pore size of the oxide depends on the micellar size and varies with the alkyl chain length of the surfactant used. The total porosity also varies with the amount of surfactant used. Thus the pore size and pore volume can be closely controlled by accordingly choosing the size of the micelles and their concentration.

In broad outlines this paper discusses the method of preparation of γ Al_2O_3 membranes of controlled pore sizes ranging from 50–60 Å, and total porosity of 0.29–0.36 cm^3/gm by incorporating surfactant micelles acting as poreformers. The pore structure, as studied by nitrogen adsorption and transmission electron microscopy, and their relation to the micellar sizes, as studied by quasielastic light scattering has been discussed.

Rejection of polyethylene glycol solutions of molecular weights 6,000, 10,000, and 35,000 and some standard protein solutions namely bovine serum albumin, ovalbumin and lysozyme which have molecular weights 67,000, 43,000 and 14,300 through these membranes have also been studied.

The percentage rejection data obtained were explained using the existing models developed by Sourirajan and Matsuura [5] and later modified by Brites and de Pinho (6).

2. Experimental

2.1. Materials

The materials used in the experiment were:

(1) Sintered alumina discs of 25 mm diameter and 1 mm thickness having apparent porosity 35% (determined by water displacement method) as supports for the membranes from Sudarshan Electricals, India.

(2) Aluminium secondary butoxide (ASB) with alumina content 21% from Fluka.

(3) Secondary butanol of spectroscopic grade from SRL, India.

(4) Double distilled water.

(5) Concentrated nitric acid.

(6) Dodecyl trimethyl ammonium bromide (DTAB), of 98% purity from Fluka.

(7) Tetradecyl trimethyl ammonium bromide (TTAB), of 98% purity from Fluka.

(8) Hexadecyl trimethyl ammonium bromide (CTAB), of 98% purity from Fluka.

(9) Polyethylene glycol (PEG) of mol. wts. 35, 10, and 6 kD from SRL India Ltd.

(10) Bovine serum albumin (BSA) from Loba Chemie, India.

(11) Lysozyme (LY) from SRL, India Ltd.

(12) Ovalbumin (OV) from Sigma.

(13) Membrane holder from Toplite Pvt. Ltd., India.

2.2. Sol preparation

Aluminium secondary butoxide (ASB) was dissolved in 2 butanol (2 moles/litre) and then hydrolyzed with aqueous solutions of surfactants (15–45 mM) following the Yoldas process [4, 7, 8]. The temperature was maintained at 80 °C and vigorous stirring was performed during hydrolysis. The gel resulting from hydrolysis was peptized to a translucent sol with concentrated HNO_3. The surfactants used were of the quaternary ammonium bromide series and the amount of surfactant added was varied from 15–45 mM. The CMCs of these surfactants in water are 15×10^{-3} moles/litre, 3.5×10^{-3} moles/litre and 0.92×10^{-3} moles/litre for DTAB, TTAB and CTAB respectively.

2.3. Coating experiments

The various sols made were used to coat sintered alumina supports which were discs of 25 mm diameter and 1 mm thickness. The porosity of the support was about 35% and the average pore size was 1 μm. Prior to coating the supports were polished with fine emery paper and washed with acetone in an ultrasonic bath. Coating was done by spinning, maintaining the sol viscosity 2 to 3 cP by solvent evaporation or addition, and at a spinning speed of 2000 rpm. These were subsequently dried in atmosphere for 24 h and fired at the rate of 1°C per minute to 600 °C for 2 h.

In order to establish the reproducibility of results at least three batches of sol of same composition were prepared and three membranes from each batch were coated. Among these one from each batch composition was used for further characterization.

2.4. Pore size measurements

Pore size of the membranes was determined by nitrogen adsorption measurements using the Horvath-Kawazoe (HK) method. Nitrogen adsorption measurements were done in a Micromeritics instrument using the ASAP 2000 programme, which gave the pore size distribution of the samples as well as the average pore size and pore volume. The sample was degassed for 10 h at 210 °C to 15 μm Hg vacuum prior to analysis. The sample was

maintained at liquid nitrogen temperature throughout the analysis. A maximum relative pressure of 0.9989 could be achieved at this temperature. The cut-off pore size was 15 Å on the lower side and 1000 Å on the higher side.

2.5. Microstructure studies by TEM

Transmission electron microscopy was performed on a Hitachi H 600 for study of pore size and pore morphology. Samples of CTAB, TTAB and DTAB templated aluminas were ground to fine powders and dispersed in isopropanol by ultrasonication for 15 min at 200 W power and then allowed to settle for about half an hour. A drop of the supernatant liquid from this suspension was then placed on the carbon coated TEM grids of 200 mesh with the help of a micropipette. The solvent in the sample was evaporated by exposing it to the atmosphere for a few hours. The dried sample was then placed in the TEM sample chamber for microscopy. The voltage used was 75 kV.

2.6. Micellar size determination by QELS

The boehmite sols prepared by hydrolysis of alkoxides and containing surfactant micelles were analyzed using quasi elastic light scattering which gave particle size distribution of the surfactant micelles as well as the γ AlOOH particles in the sol. The instrument used was Brookhaven BI-90 particle sizer having a 50 mm path length and a laser beam of 30 MW. The resolution of the instrument was 0.5–100 nm. MilliQ water was used for preparing the sols and all ingredients were filtered through a 0.2 μm filter before the analysis. Utmost care was taken to avoid dust particles contaminating the sol while preparation or analysis.

2.7. Permeability measurements

Fluxes of pure water and standard solutes namely PEG 35,000, 10,000, and 6,000 and proteins BSA, OV, and LY were determined in the permeability set up shown in Fig. 1. The set up consists of a permeability measurement cell or the membrane holder, a reservoir for storing the liquid and a pressure gauge for measuring the pressure at inlet. Pressurized liquid is fed from the top surface of membrane by maintaining a constant pressure with the help of compressed gas on the liquid column in the reservoir. The flow rate is determined by measuring the volume of liquid collected at the outlet in a given time interval.

When there was drop in the flux of the membrane due to repeated use and fouling, the membrane was regenerated by firing to 600 °C. Such regeneration could be done successfully upto at least 3/4 times.

The circular disc membrane of 25 mm diameter is fixed between two hollow conical stainless steel parts having 2 mm flat rims as shown in the inset in Fig. 1. The lower one is 2–3 mm larger in diameter than the upper one and has a 5 mm deep groove with a flat rim on which the membrane, the silicone gaskets as well as the upper part of the holder rests. These are all further held together tightly by a connector nut.

2.8. Measurement of feed and permeate concentrations

The concentrations of the PEG feed and permeate solutions were measured by the method of Sims and

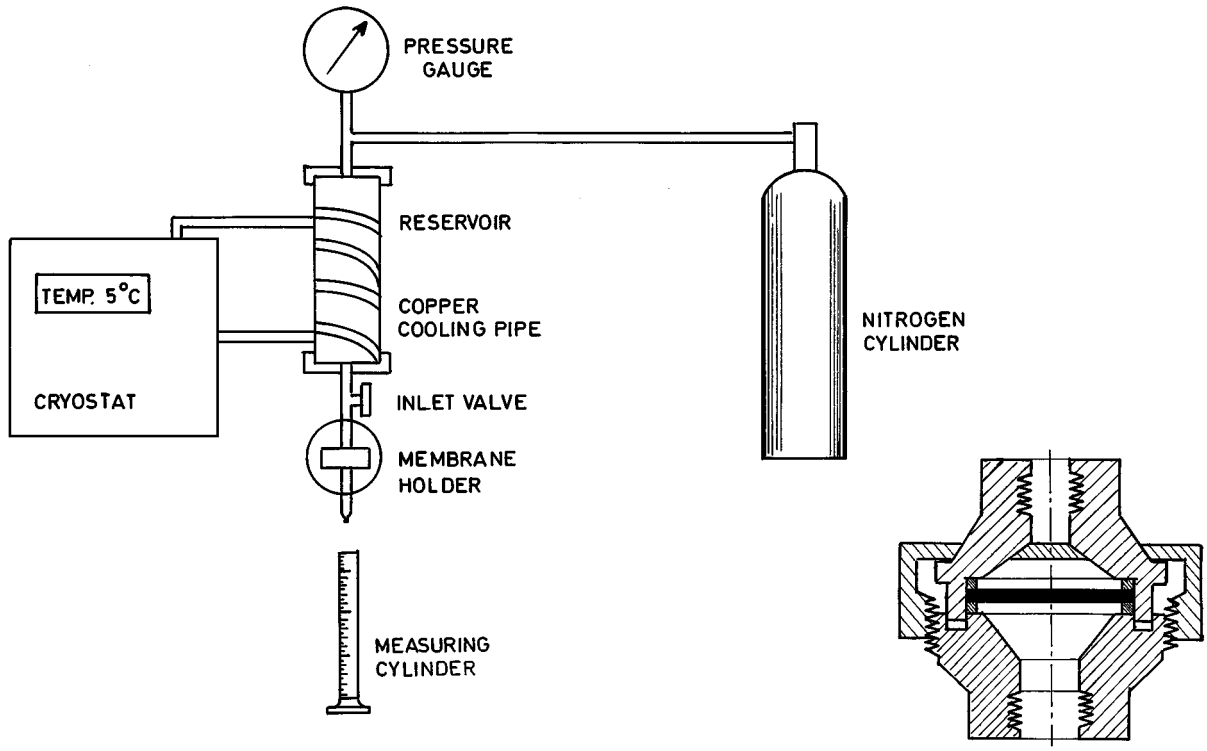

Figure 1 Schematic diagram of the permeability testing apparatus.

Snape [9]. According to this method, 4 ml of the PEG containing sample was mixed thoroughly with 1 ml of each of the reagent A (5% $BaCl_2$ in 1 N HCl) and reagent B (0.127 g I_2 + 0.4 g KI + 100 ml water). The sample was allowed to stand for 20 min followed by measurement of the sample absorbance at 535 nm. The sample absorbance was then compared with a previously obtained calibration plot of absorbance versus concentration of standard solutions. This method is applicable only for very dilute solutions of typically below 20 ppm. Hence some feed and permeate solutions were diluted accordingly before analysis.

The protein concentrations in the feed and permeate solution were determined spectrophotometrically by UV absorbance measurements at 280 nm using a Shimadzu 160 UV spectrophotometer.

2.9. Measurement of tortuosity of membranes

Tortuosity of membranes was calculated from the apparent conductivity of a 0.6 M KCl solution measured across the membrane and the true specific conductivity of the same obtained from the literature, using the relation [10]:

$$\frac{\text{apparent specific conductivity}}{\text{true specific conductivity}} = \frac{\text{porosity}\,(\varepsilon)}{\text{tortuosity}\,(k_0)}$$

3. Results and discussion

The pore sizes in the samples were measured by nitrogen adsorption using the HK method, and in order to ensure that the pores were formed by surfactant micelles acting as templates, the micellar sizes in the sol were determined using quasi elastic light scattering. The results of pore size distribution using HK method and particle size distribution of micelles by QELS are discussed in details below. TEM of the samples was also performed in order to study the pore morphology namely their shape and size and their interconnectivity.

3.1. Micellar size by QELS

The micellar sizes as determined by quasi elastic light scattering for sols containing 15 mM surfactant solutions DTAB, CTAB and TTAB are shown in Fig. 2a, b and c respectively. The particle size plots show a bimodal distribution for all cases. The larger peak between 10–100 nm indicates the presence of sol particles of γ AlOOH, while the smaller one below 10 nm signifies the micelles. The micellar sizes as seen from the smaller peak in Fig. 2a, b and c are 4, 3.6 and 3 nm for CTAB, TTAB and DTAB respectively. The size of CTAB micelles measured by X-ray diffraction at 26% surfactant concentration and 27 °C, is 45 Å as reported by Ekwall *et al.* [11]. Fig. 2d shows the particle size distribution of a sol with no surfactant.

3.2. Pore size distribution: surfactant effect

The pore volume vs. pore diameter plots (Fig. 3) as calculated from the N_2 adsorption isotherms for the various samples show that a sol containing DTAB (curve D) gives pores of average diameter 50 Å, a sol containing TTAB (curve T) gives pores of average diameter 55 Å, while a sol containing CTAB (curve C) gives pores of average size 60 Å. All these sols were made

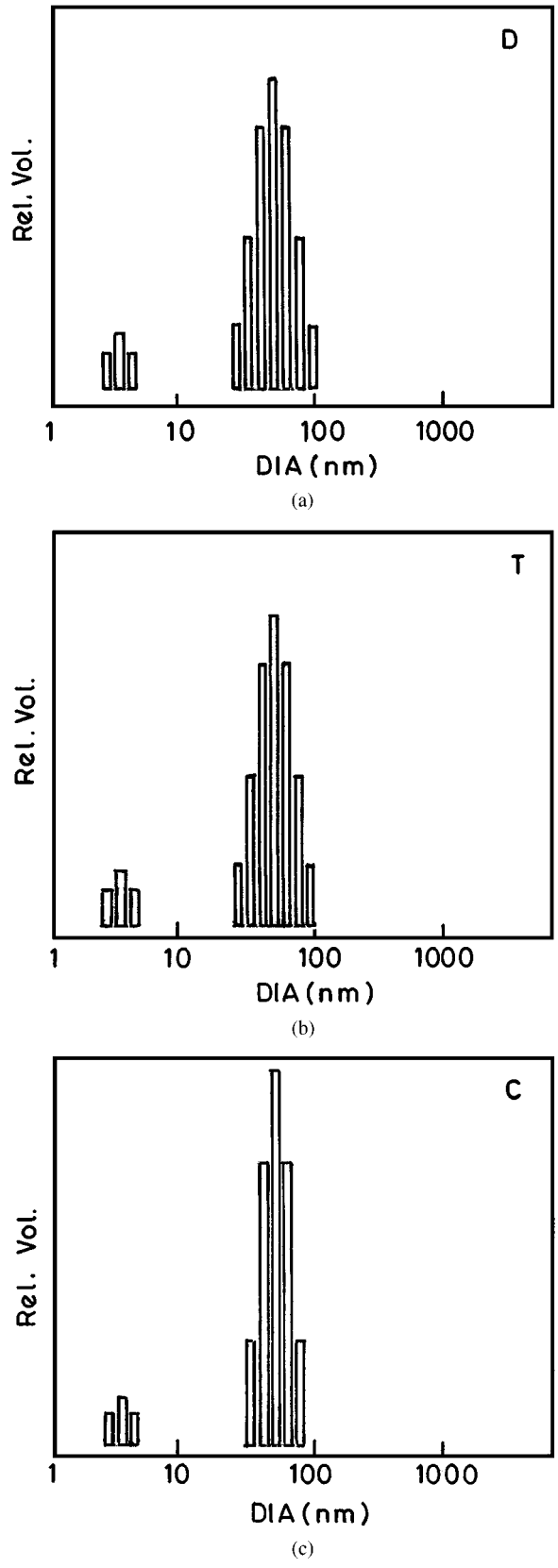

Figure 2 Particle size distribution of (a) DTAB (15 mM), (b) CTAB (15 mM) and (c) TTAB (15 mM) incorporated alumina sol as obtained by QELS. The peak below 10 nm is for the micelles whereas that between 10–100 nm is for the sol particles.

TABLE I Comparison of pore volumes determined from N_2 adsorption and calculated micellar volumes from QELS data (surfactant effect)

Surfactant	Pore volume (cm^3/gm)	Micellar size (nm)	Micellar volume (cm^3/gm)	Micellar volume + Pore volume of non-templated membrane (cm^3/gm)
None	0.14	—	—	—
DTAB	0.29	3.0	0.09	0.23
TTAB	0.32	3.6	0.14	0.28
CTAB	0.36	4.0	0.19	0.33

TABLE II Comparison of pore volumes determined from N_2 adsorption and calculated micellar volumes from QELS data (concentration effect)

CTAB concentration (mM)	Pore volume (cm^3/gm)	Micellar volume (cm^3/gm)	Micellar volume + Pore volume of non-templated membrane (cm^3/gm)
15	0.32	0.19	0.33
20	0.36	0.26	0.40
45	0.69	0.59	0.73

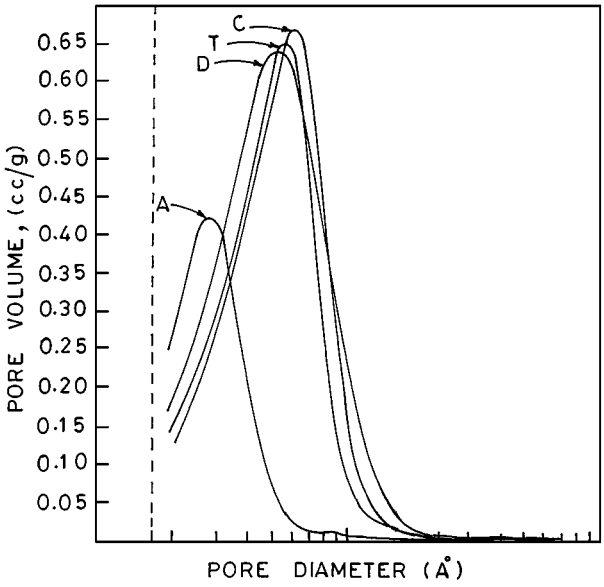

Figure 3 Pore size distribution in 15 mM CTAB (C), TTAB (T) and DTAB (D) templated membranes as obtained by nitrogen adsorption measurements. Pore size distribution in γ Al_2O_3 membranes (A) without any surfactant incorporation is also shown here for comparison.

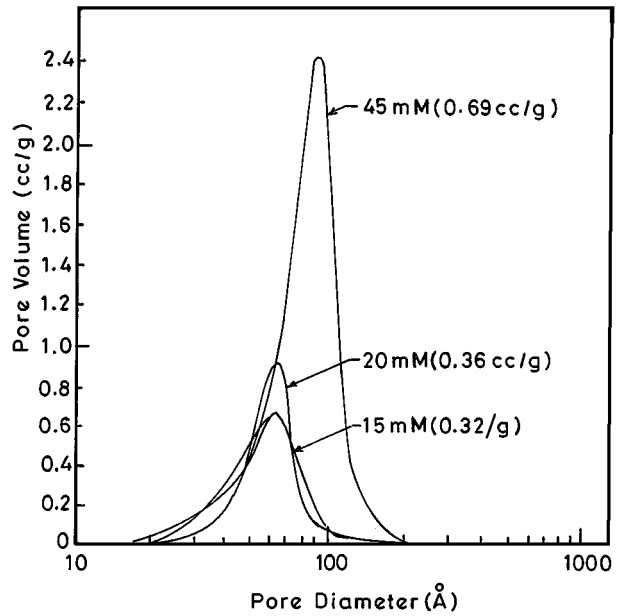

Figure 4 Pore size distribution in 15, 20 and 45 mM CTAB templated membranes as obtained by nitrogen adsorption measurements.

by hydrolyzing alkoxides with 15 mM solutions of the above surfactants. The pore volume in these samples were 0.29, 0.32 and 0.36 cm^3/gm for DTAB, TTAB and CTAB respectively as obtained from nitrogen adsorption. Curve A of Fig. 3 shows the pore size distribution in a sample made from a sol containing no surfactant has average pore size 25 Å and pore volume 0.14 cm^3/gm.

The calculated micellar volumes for 15 mM concentrations of the above surfactants using QELS data of micellar sizes were 0.09, 0.14, 0.19 cm^3/gm for DTAB, TTAB and CTAB respectively. On adding the pore volume of a non-templated membrane i.e. 0.14 cm^3/gm to micellar volume, the total calculated pore volumes were 0.023, 0.28 and 0.33 cm^3/gm for DTAB, TTAB and CTAB respectively, which are very close to experimental values obtained from HK plots as shown in Table I.

3.3. Pore size distribution: concentration effect

On increasing the amount of surfactant to 20 and 45 mM, it was found that the total pore volume of the membranes increases in accordance with micellar volume. The total pore volumes in the three samples with 15, 20 and 45 mM CTAB were 0.32, 0.36 and 0.69 cm^3/gm as obtained from nitrogen adsorption measurements. The calculated micellar volumes for these concentrations of surfactants were 0.19, 0.26 and 0.59 cm^3/gm. On adding the pore volume of non-templated samples to the calculated micellar volumes, the total theoretical pore volume was obtained as 0.33, 0.40 and 0.73 cm^3/gm, which agree with the experimental data as shown in Table II.

Fig. 4 shows pore size distribution of alumina samples hydrolyzed with 15, 20 and 45 mM CTAB solutions (curve C) and 25 mM solution of DTAB (curve D). It can be seen that the average pore sizes in the 15 and 20 mM samples were both 60 Å, whereas in the 45 mM sample was 85 Å. The increase in pore size at very high surfactant concentration may be due to pore coalescence and multimicellar interactions.

Adsorption-desorption isotherms (Fig. 5) of N_2 show well defined hysteresis for all samples in which surfactant templating was done. However, the one without any surfactant showed a negligible hysteresis.

3.4. TEM studies

The TEM micrographs of the samples show a highly porous networked structure as seen in Fig. 6a, b and c. All the samples showed more or less a similar pore morphology except for the difference in their average pore sizes as studied by optical microscopy of the TEM negatives. Table III shows pore size measurements of

TABLE III Measurement of pore sizes from TEM micrographs using an optical microscope

Sample	TEM magnification	Optical microscope magnification	Mean pore diameter (Å)
DTAB	×80,000	×20	50.2
TTAB	×80,000	×20	55.6
CTAB	×80,000	×20	60.9

TABLE IV Pure water fluxes for DTAB, TTAB and CTAB membranes

Membrane templated with	Δp kPa	v (calculated) m/s $\times 10^8$	v (experimental) m/s $\times 10^8$
CTAB	103	5.06	5.26
DTAB	103	3.51	4.05
CTAB	137	6.73	7.63
DTAB	137	4.67	5.18
CTAB	172	8.45	10.2
DTAB	172	5.87	6.45

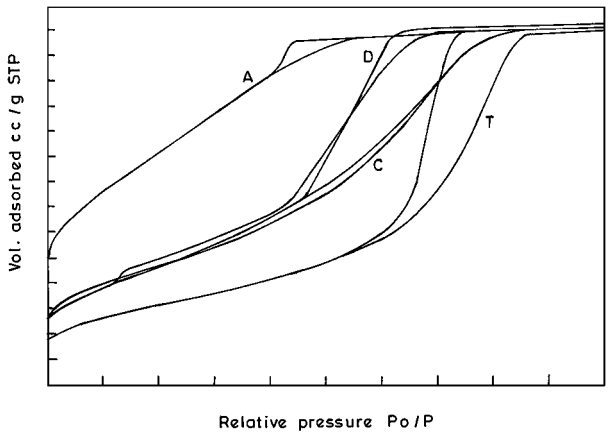

Figure 5 Adsorption-desorption isotherms of nitrogen for CTAB (C), TTAB (T), DTAB (D) templated membranes and also for non-templated membranes. Templated membranes show a well defined hysteresis while the non-templated membrane (A) shows a negligible hysteresis.

various samples from TEM micrographs by means of a scale fitted to the eye piece of the microscope. The scale in the eye-piece was earlier calibrated. Mostly circular pores of sizes varying from 40–70 Å could be viewed. However, some pores showed an elongated slit shaped structure which seemed to rise from coalescence of two or more pores. The average pore size measured in CTAB samples was 60.9 Å, for TTAB it was 55.6 Å and for DTAB it was 50.2 Å.

3.5. Pure water flux

Permeability measurements with pure water and standard solutes were done for DTAB and CTAB membranes. Pure water flux through the DTAB and CTAB membranes were determined at 15, 20 and 25 psig feed pressures. These values are shown in Table IV and Fig. 7. It was seen that at the same pressure, flux through CTAB membranes was more than that through DTAB. CTAB membranes gave pure water fluxes $5.26 \times 10^{-8}, 7.63 \times 10^{-8}$ and 10.2×10^{-8} m/s at 15, 20 and 25 psig feed pressures respectively, whereas DTAB membranes gave fluxes 4.05×10^{-8}, 5.18×10^{-8} and 6.45×10^{-8} m/s at the respective pressures.

TABLE V Rejection of standard solutes through CTAB and DTAB membranes at 25 psig feed pressure

Membrane	Solute	Mol. wt. (kD)	Feed (abs.)	Permeate (abs.)	λ at max abs. nm	% Rejection
CTAB	BSA	67	0.601	0.004	280	99+
	OV	43	0.717	0.501	280	93.0
	LY	14.3	2.501	0.332	280	86.7
	PEG	35	0.581	0.004	535	87.1
	PEG	10	0.296	0.128	535	56.7
	PEG	6	0.692	0.528	535	23.7
DTAB	BSA	67	0.620	0.006	280	99+
	OV	43	0.732	0.029	280	96.0
	LY	14.3	2.503	0.155	280	93.8
	PEG	35	0.482	0.007	535	96.5
	PEG	10	0.296	0.037	535	87.5
	PEG	6	0.692	0.229	535	66.9

3.6. Rejection of standard solutes

Solutions of polyethylene glycol (PEG) of molecular weights 35,000, 10,000, and 6,000 of approximately 10 ppm concentrations, and 1 mg/ml of each of the proteins BSA, OV and LY, when used as feed for the above membranes showed rejections in case of DTAB and CTAB membranes that are listed in Table V. The rejection vs. molecular weight plots for the two membranes show sharp drops at mol. wts. 14.3 and 10 kD respectively at a little lower than 90% rejection value as shown in Fig. 8. Hence, it can said that the "molecular weight cut off" for DTAB membrane is about 10 kD whereas for the CTAB membrane it is about 14 kD.

3.7. Explanation and fitting of experimental data using existing models

Carman Kozeny's law [10] is the basic law used to describe the flow through a porous media:

$$v = \frac{\varepsilon m^2 \Delta p}{\left(2\omega k_0^2\right) L \eta} \tag{1}$$

where Δp is the driving pressure, η is the viscosity of the solution. The other parameters are related to the morphology: ε is the porosity, m is the mean hydraulic radius given as $\varepsilon/\{S_0(1-\varepsilon)\}$, where S_0 is the specific surface area of the medium, ω is the pore circularity factor, τ is the tortuosity and L is the thickness of the membrane. Pure water fluxes were calculated using the Kozeny Carman equation. ε is 0.52 as obtained from HK data, m is pore diameter/4 which is 15 and 12.5 Å in case of CTAB and DTAB membranes respectively, Δp is the differential pressure which was 25 psig or 172 kPa, ω is the pore circularity factor taken as 1.05 (10) for pores of elliptical shape (with $a = 2b$), τ is the tortuosity the average value of which is 4.37 as determined experimentally, L is the thickness of the membrane which was 7 μm and η is the viscosity of

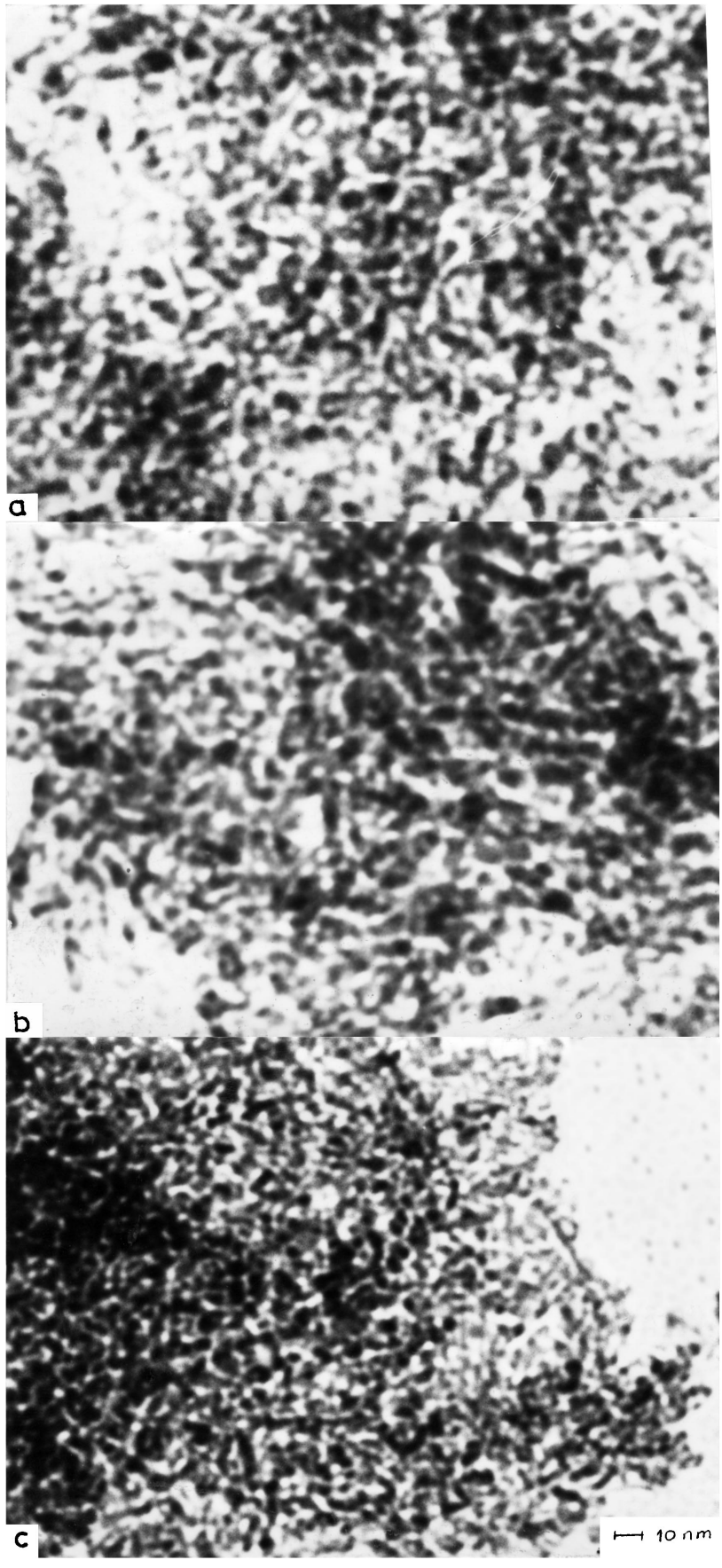

Figure 6 Transmission electron micrograph of the pore morphology of (a) CTAB, (b) TTAB, and (c) DTAB templated membranes.

the permeating liquid taken as 0.891 cP at 25 °C. The experimental values are close and show a similar trend as the calculated values as seen in Fig. 7.

A more comprehensive model (surface force-pore flow model) applied for calculating flux and rejection values in ultrafiltration of dilute to semidilute solutions through porous membranes was first proposed by Matsuura and Sourirajan [5]. It takes into account solute size, pore diameter, solute membrane/solvent friction and solute/membrane interactions. Based on a force

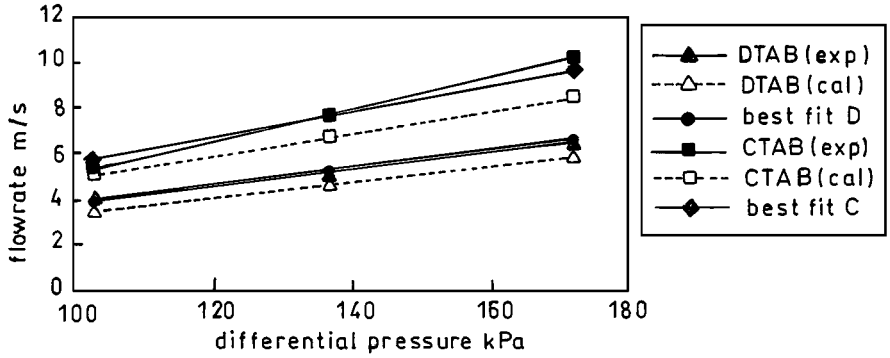

Figure 7 Pure water fluxes plotted against differential pressure as obtained experimentally (—) and by using the Kozeny Carman equation(– – –).

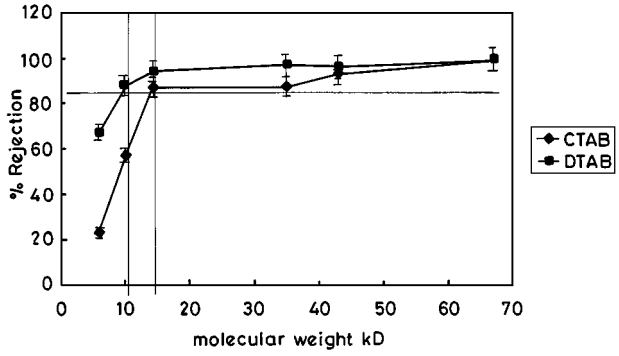

Figure 8 Experimental rejection values for the PEGs and proteins as a function of molecular weight of the solute showing "MWCO" of membranes.

balance theory proposed by Speigler [12] they assumed that inside the pore of a membrane the thermodynamic forces acting on the solute are balanced by the mechanical frictional forces. Thus,

$$F_s(r, z) = -[F_{sw}(r, z) - F_{sm}(r, z)] \tag{2}$$

Force F_s is proportional to the chemical potential gradient and each of the forces F_{sw} and F_{sm} are proportional to the relative velocities of the solute and solvent and solute and membrane with proportionality constants f_{sw} and f_{sm} respectively. Thus they had obtained the expression for flux as

$$J = \frac{\left[\frac{RT}{f_{sw}}\left(\frac{dC_s(r,z)}{dz}\right)\Big|_{r=r} + C_s(r, z)v_w(r)\right]}{\left(1 + \frac{f_{sw}}{f_{sm}}\right)} \tag{3}$$

with the boundary conditions

$$z = 0, \quad C_s(r, 0) = C_{sm} \tag{4}$$

$$z = L, \quad C_s(r, L) = C_{sp}(r) \tag{5}$$

and

$$C_{sp} = \frac{J(r)}{v_w(r)} \tag{6}$$

The differential Equation 3 together with 4, 5 and 6 for the boundary conditions yield the solution

$$C_{sp}(r) = \frac{C_{sm}\exp\left(\frac{f_{sw}v_w(r)L}{RT}\right)}{1 + \left[b\exp\left(\frac{f_{sw}v_w(r)L}{RT}\right) - 1\right]} \tag{7}$$

Brites and de Pinho [6] use this model to predict the ultrafiltration performance at different operating conditions and for membranes of various pore sizes and pore size distributions using polyethylene glycol solutions. After introduction of the dimensionless variables ρ and α (r), where,

$$\alpha = \{v_w(r)L f_{sw}\}/RT = \{2v_{w\,av}(1 - \rho^2)L f_{sw}\}/RT,$$
$$\rho = r/R_p \quad \text{and} \quad b = (f_{sw} + f_{sm})/f_{sw},$$

and assuming Poiseuille flow and averaging the concentration given by Equation 6 they had obtained the rejection as

$$R' = 1 - \frac{\int_0^1 \frac{\exp\alpha(\rho)}{1 + b[\exp\alpha(\rho) - 1]}\alpha(\rho)\rho\, d\rho}{\frac{\Delta P R_p^2}{16\mu D_{sw}}} \tag{8}$$

Assuming a normal distribution of pore radius, $F(R_p)$, with $\bar{R}_p$ and σ being the average pore radius and standard deviation respectively, the Equation 7 is rewritten as

$$R' = 1 - \frac{\int_{\bar{R}_p - 2\sigma}^{\bar{R}_p + 2\sigma}\left[F(R_p) \times \int_0^1 \frac{\exp\alpha(\rho)}{1 + b[\exp\alpha(\rho) - 1]}\alpha(\rho)\rho\, d\rho\right]dR_p}{\frac{\Delta P}{16\mu D_{sw}}\int_{\bar{R}_p - 2\sigma}^{\bar{R}_p + 2\sigma} F(R_p)R_p^2\, dR_p} \tag{9}$$

Equation 9 was used in the present work to calculate values of rejection. On integration of the above expression, an equation in terms of b and c was obtained by us and substitution of two sets of experimental values gave two such independent equations which were solved to obtain the values of b and c. From b and c, the values of f_{sw} and f_{sm} were calculated by us as shown in Table VI. It can be seen from Table VI that with increase of molecular weight of the solute, f_{sw} increases, but f_{sm} decreases. This may be due to the difference in the nature and magnitude of the frictional forces between solute-water and solute-membrane, which may arise because of two reasons mainly. Firstly because of water of hydration around the solute molecules, and secondly since water molecules are very small compared to solute molecules, the total frictional force between solute-water F_{sw}, is more dependent on surface

TABLE VI Calculated values of friction coefficients f_{sm} and f_{sw}

Solute (s)-solvent (w)	Membrane (m)	Friction factors $f_{sw\times 10}^{-14}$	Friction factors $f_{sm\times 10}^{-14}$
PEG 6 kD-water	Alumina	8.93	4.47
PEG 10 kD-water	Alumina	9.24	4.16
PEG 35 kD-water	Alumina	10	3.51
Ly 14.3 kD-water	Alumina	9.83	3.93
BSA 67 kD-water	Alumina	12.6	1.26

TABLE VII Comparison of calculated and experimental rejection values obtained for PEGs and proteins

Solute	Membrane pore size (Å)	Experimental value of rejection	Calculated value of rejection
PEG 6 kD	30 (CTAB)	23.7	30.18
PEG 6 kD	25 (DTAB)	66.9	51.5
PEG 10 kD	30 (CTAB)	56.7	65.6
PEG 10 kD	25 (DTAB)	87.5	76.1
PEG 35 kD	30 (CTAB)	87.1	87.3
PEG 35 kD	25 (DTAB)	96.5	91.7
LY	30 (CTAB)	86.7	88.6
LY	25 (DTAB)	93.8	90.1
OV	30 (CTAB)	93.0	—
OV	25 (DTAB)	96.0	—
BSA	30 (CTAB)	99+	99.8
BSA	25 (DTAB)	99+	99.9

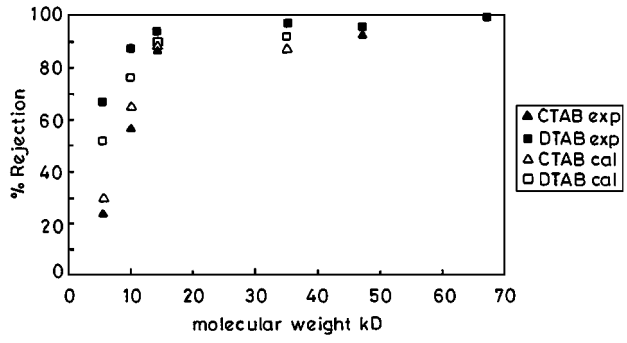

Figure 9 Experimental rejection values for the PEGs and proteins as a function of molecular weight of the solute to the calculated values obtained by the pore flow model.

area of the solute molecule in contact with water, rather than the solute mol. wt., whereas the total frictional force between solute-membrane, F_{sm} is dependent on solute mol. wt.

On substitution of f_{sw} and f_{sm} the calculated values for the rejection R' were obtained. These values are compared with the experimental values as shown in Table VII and Fig. 9. It can be seen that this model gives an excellent fit for the experimental data with solutes of different molecular weights for both the CTAB and DTAB membranes having different pore size distributions.

4. Conclusion

γ Al_2O_3 membranes of closely controlled pore sizes to the extent of 5 Å and average pore size 50–60 Å were successfully prepared for the first time by surfactant templating method. Surfactants were incorporated in the alumina sol by dissolving them in water above their critical micellar concentration and using them to hydrolyze aluminium alkoxides. 15 mM solutions of quaternary ammonium surfactants namely DTAB, TTAB and CTAB were found to give pore sizes of 50, 55 and 60 Å respectively. The reproducibility of the results was established by repeating the measurements two to three times that showed deviation within 1%. Thus, for an increase of every two carbon atoms in the alkyl chain length of the surfactant, the average pore size increased by 5 Å. These pore sizes also matched with the micellar sizes obtained by quasi elastic light scattering. Moreover, it was also found that the pore volume increases or decreases with increase or decrease of the amount of surfactant.

The surfactant templated membranes can be successfully used for ultrafiltration of proteins and can be of importance in downstream biotechnology processes. The experimental values of rejections for PEGs of 6, 10 and 35 kD and standard proteins namely BSA (67 kD), OV (43 kD) and LY (14.3 kD) showed a reasonably good agreement with calculated values using the pore flow model developed by Sourirajan and Matsuura [3] and later modified by Brites and de Pinho [6].

Another outstanding advantage exploited in the ultrafiltration studies of ceramic membranes was that once fouled membranes could be easily made to regain their properties as regards to flux and rejection by simply firing the membrane to 600 °C. Thus the common problem of fouling and related flux reduction could be handled without discarding the membrane.

References

1. C. T. KRESGE *et al.*, Nature **359** (1992) 710–712.
2. G. D. STUCKY *et al.*, *ibid.* March (1994).
3. P. T. TANEV and T. J. PINNAVAIA, *Science* **271** (1996).
4. B. E. YOLDAS, *J. App. Chem. Biotech.* **23** (1973) 803–809.
5. T. MATSUURA and S. SOURIRAJAN, *Ind. Eng. Chem. Process Des. Dev.* **20** (1981) 273.
6. A. M. BRITES and M. N. DE PINHO, *J. Membrane Sci.* **78** (1993) 265.
7. B. E. YOLDAS, *Ceram. Bull.* **54**(3) (1975a) 289–290.
8. *Idem., J. Mater. Sci.* **10** (1975b) 1856–1860.
9. G. E. C. SIMS and T. J. SNAPE, *Anal. Biochem.* **107** (1980) 60.
10. P. C. CARMAN, in "Flow of Gases through Porous Media" (Butterworths Scientific Publications, London, 1981) pp. 46–47.
11. P. EKWALL, L. MANDELL, P. SALYOM, *J. Colloid Interface Sci.* **35** (1971) 519.
12. K. S. SPEIGLER, *Trans. Faraday Soc.* **53** (1957) 1408–1428.

Received 12 February 1998
and accepted 24 February 1999